Dalton Transactions

PAPER

View Article Online
View Journal | View Issue

Open Access Article. Published on 18 August 2016. Downloaded on 11/12/2024 11:02:41 PM.
This article is licensed under a Creative Commons Attribution-NonCommercial 3.0 Unported Licence.

Cite this: *Dalton Trans.*, 2016, **45**, 16789

Improving selectivity in catalytic hydrodefluorination by limiting S_NV reactivity†

Juliane Krüger,[a] Christian Ehm*[b] and Dieter Lentz*[a]

Received 26th July 2016,
Accepted 17th August 2016

DOI: 10.1039/c6dt02961b

www.rsc.org/dalton

Catalytic hydrodefluorination of perfluoroallylbenzene with Cp_2TiH in THF is unselective and yields a variety of previously unknown compounds, predominantly activated in the allylic position. Several different mechanisms have been examined in detail using solvent corrected (THF) DFT(M06-2X) calculations for the archetypal perfluorinated olefin perfluoropropene and perfluoroallylbenzene: (a) single electron transfer, (b) hydrometallation/fluoride elimination, (c) σ-bond metathesis (allylic or vinylic), and (d) nucleophilic vinylic substitution (S_NV, w/o Ti–F contacts in the TS). S_NV is shown to be a competitive mechanism to hydrometallation and proceeds *via* ionic species from which F-elimination is facile and unselective leading to low selectivity in polar solvents. Subsequent experiments show that selectivity can be increased in a non-polar solvent.

Introduction

Fluoroorganic compounds have received increasing attention because of their unique properties especially in the fields of pharmaceuticals, agricultural chemistry and materials science.[1–11] However, the carbon–fluorine bond is the strongest and the most unreactive bond found in organic molecules and its use as an active functional group is a significant chemical challenge.[12,13] A growing number of scientific publications have focused on transition metal-catalyzed C–F bond activation and C–F bond functionalization.[14–18,19–25] Several reviews on the current state of the art in early and late transition metal catalyzed C–F bond activation have been published.[14–17,26–30] For the simplest kind of C–F bond activation, hydrodefluorination (HDF), a feasible and promising strategy is to use transition metal hydrido complexes.[29,31–48] Several systems capable of catalytic HDF are known, often using expensive late transition metal compounds.[28,36,42,43,47–53] Only a few examples of group 4 catalyzed processes are known; Rosenthal *et al.* and Crimmin *et al.* described a zirconium based catalytic system using alanes as hydride sources.[35,47] Recently we published an updated catalytic cycle for an earlier reported HDF employing a commercially available and air-stable precatalyst (titanocene difluoride, **1a**) and a comparatively inexpensive hydride source (diphenylsilane, **2**).[54] The active species, a titanocene(III) hydrido complex (**1**), is generated in trace amounts *in situ* from **1a** and **2** as catalyst regeneration with **2** is endergonic; the resting state is the trimeric titanocene(III) fluoride. *E*/*Z* regioselectivity in catalytic olefinic HDF using **1** appears to be substrate dependent but often unselective while vinylic C–F activation is always strongly preferred over allylic C–F activation.[46] Based on experimental selectivities a hydrometallation/elimination mechanism (HM/E) and σ-bond metathesis (SBM) were proposed to be competing mechanisms but the reason for the pronounced substrate effect on regioselectivity remained elusive. Some group $4d^0$ systems have been studied theoretically. The groups of Jones and Eisenstein described the defluorination of perfluoropropene using tetravalent $Cp^*_2ZrH_2$ and Cp^*_2ZrHF complexes.[55] The first vinylic C–F bond exchange occurs *via* an internal insertion of the olefin followed by β-F elimination (HM/E mechanism).

In the following, we will give new experimental and computational insights into the mechanism and regioselectivity of HDF reactions of catalyst **1** with hexafluoropropene (**3**) and perfluoroallylbenzene (**4**) and show that the solvent choice has a marked influence on HDF regioselectivity.

Results and discussion

In earlier experiments with substrate **3** and catalyst **1** we observed the following experimental trends: (a) temperature changes (−25 to +25 °C) do not influence the observed product selectivity,[56] (b) steric and electronic changes in the catalyst influence its activity but barely influence the selectivity (*E*/*Z* 0.67 to 1.07 for **3**), (c) changing the substrate has tremendous influence on both activity (TOF) as well as the selectivity (*e.g.*

[a]*Institut für Chemie und Biochemie, Anorganische Chemie, Freie Universität Berlin, Fabeckstr. 34-36, 14195 Berlin, Germany. E-mail: dieter.lentz@fu-berlin.de*
[b]*Dipartimento di Scienze Chimiche, Università di Napoli Federico II, Via Cintia, 80126 Napoli, Italy. E-mail: christian.ehm@unina.it*

†Electronic supplementary information (ESI) available. See DOI: 10.1039/c6dt02961b

Open Access Article. Published on 18 August 2016. Downloaded on 11/12/2024 11:02:41 PM.
This article is licensed under a Creative Commons Attribution-NonCommercial 3.0 Unported Licence.

Table 1 Experimental product selectivity (solvent: diglyme)

Substrate	**3**[39]	**5**[46]	**6**[46]
E : *Z* ratio	2 : 3	14 : 1	1 : 16

1,1,1,3,3-pentafluoropropene (**5**) and 1,1,2-trifluorovinyl-ferrocene (**6**) in Table 1) and (d) the choice of silane for the regeneration reaction has no influence on the selectivity but does influence the activity.[46] The low selectivity observed with **1** differs notably from selective HDF of **3** using Zr(IV).[55]

Mechanistic studies on the HDF of fluoroolefins

Solvent corrected (PCM:THF) mechanistic DFT studies were performed on the M06-2X/TZ//M06-2X/DZ level of theory, see the Experimental section for details.[57]

In the following we will first analyze HDF pathways for **1** and the archetypical olefin **3** before presenting results for substrate **4**.

Several different mechanisms are possible and all have low activation barriers; TS formation proceeds directly from the reactants as the SOMO blocks the vacant coordination site of **1** rendering the formation of all adducts (or contact pairs) of **3** and **1** endergonic.[58,59] HM/E (type A TS), S_NV[60] (type B TS), 4-center-SBM, 6-center-SBM (type C TS) as well as SET were considered to play a role.

Hydrometallation/elimination pathway

In plane approach of the catalyst towards the substrate C=C double bond (hydride attack at C1) *via* 4-membered **TS$_A$3-5d** (+8.5 kcal mol^{-1}) leads to HM product **5d** (−38.8 kcal mol^{-1}).[61] The barrier is purely entropic. **5d** possesses no metal fluoride interactions and a staggered conformation (Fig. 1). HM is irreversible. IRC scans show that C–H bond formation is completed before Ti–C bond formation starts noticeably (see the ESI†). Rotamers **5a–5c** have β-F dative interactions (Fig. 2). A β-H-agostic conformation could not be found. Interconversion between the resting states (RS) **5a–5c** *via* **5d** is

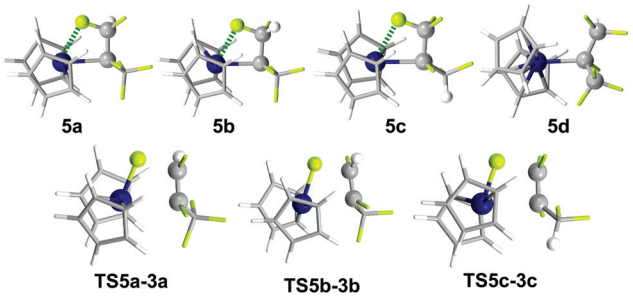

Fig. 2 Resting states (RS) and elimination TS within the HM/E pathway.

easy as the energy difference between the RS is <4 kcal mol^{-1} and thus the ratio of the formed products depends only on $\Delta\Delta G^{\ddagger}$ of the elimination TS (Curtin–Hammett).[62]

Barriers for F-elimination lie between 9.8 and 17.8 kcal mol^{-1} above the lowest RS **5a** and lead *via* adduct complexes with H–F contacts to the isolated products. The elimination step is also irreversible and selectivity determining. Inspection of Table 2 and Fig. 1 shows that the β-fluorine elimination TS (**TS5a-3a** to **TS5c-3c**) are energetically closer to the RS (**5a–d**) than to the products (**3a–c**; 10–18 kcal mol^{-1} from RS, >30 kcal mol^{-1} from products).[63] However, comparison of the geometries (Table 2 and Fig. 2) reveals that the elimination TS resemble the products much more than they resemble the RS. In particular, C=C bond lengths in **TS5a-3a** to **TS5c-3c** are closer to the lengths in the isolated olefins **3a–c** (+0.07 Å), *i.e.* formation of the olefin is almost complete already at the TS. Furthermore, C–F$_{EI}$ (>0.4 Å) and Ti–C bonds (>0.25 Å) are highly elongated, pointing to a large separation of titanocene fluoride and olefin in all TS (Table 2).

The large energy gain going from TS to the corresponding product (>30 kcal mol^{-1}) varies by only 3 kcal mol^{-1} for the three different pathways (Fig. 1). The $\Delta\Delta G$ of the three products (0, 2.0 and 11.0 kcal) and H–F contact pairs (0.0, 1.7 and 12.0) almost match the corresponding TS $\Delta\Delta G^{\ddagger}$ (0, 2.0 and 8.0 kcal mol^{-1}).

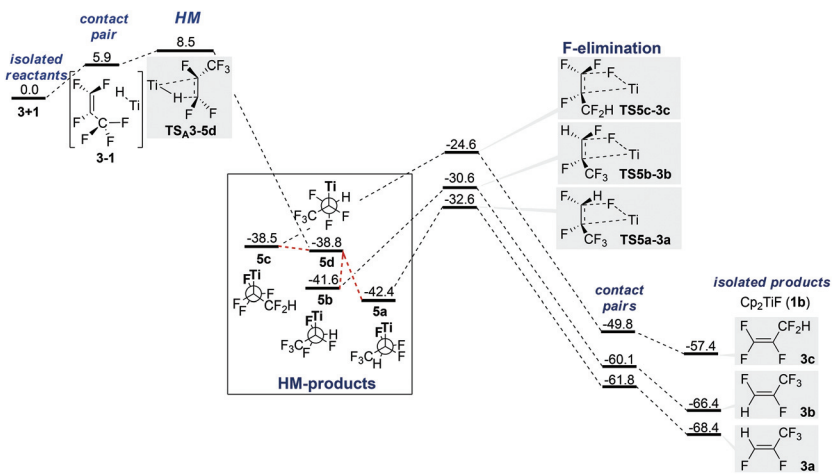

Fig. 1 PES for HM/E pathway for HDF of **3** (ΔG in kcal mol^{-1}, T = 298 K, 1 bar, in THF).

This journal is © The Royal Society of Chemistry 2016

Open Access Article. Published on 18 August 2016. Downloaded on 11/12/2024 11:02:41 PM.
This article is licensed under a Creative Commons Attribution-NonCommercial 3.0 Unported Licence.

Table 2 Selected bond distances and, relative energies in products, resting states and transition states (elimination) in Å. C–F_{El} = C–F bond length of the fluorine that is to be eliminated

	C–H	C=C	C–F_{El}	F–Ti	C–Ti	$\Delta\Delta G^a$
5a	1.090	1.501	1.427	2.292	2.324	0.0
5b	1.092	1.509	1.421	2.297	2.321	0.8
5c	1.092	1.513	1.401	2.349	2.329	3.9
TS5a-3a	1.083	1.392	1.824	2.050	2.585	0.0
TS5b-3b	1.085	1.395	1.831	2.056	2.578	2.0
TS5c-3c	1.093	1.396	1.873	2.040	2.577	8.0
3a	1.081	1.323				0.0
3b	1.084	1.324				2.0
3c	1.090	1.325				11.0
1b				1.863		

[a] With respect to the lowest ΔG in each of the three sets.

The energy difference between **3a** and **3b** has been determined experimentally by Kaiser *et al.* (−2.85 kcal mol^{-1}) and is in line with our DFT predictions.[64]

We tentatively conclude that barrier heights for elimination are dominated by product differences. Fluorinated sp^2-carbons are destabilized as fluorine prefers a strong p-character in its bonds. **TS5c-3c** is the highest TS as **3c** is destabilized by three fluorine substituents at the double bond.

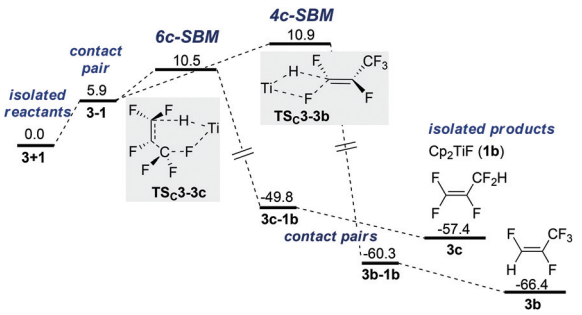

Fig. 3 PES for SBM pathways for HDF of **3** (ΔG in kcal mol^{-1}, T = 298 K, 1 bar, in THF).

Differences between **3a**/**3b** and **TS5a-3a**/**TS5b–3b**, respectively, originate from the different destabilizations that occur if a C=C double bond is destabilized by either *cis*- or *trans*-difluorination.[65–67]

σ-Bond metathesis and S_NV

An approach of Ti–H to C1 with Ti–F interaction (SBM) results in either **TS$_C$3-3b** (4-membered, +10.9 kcal mol^{-1}) or **TS$_C$3-3c** (6-membered, +10.5 kcal mol^{-1}) and leads directly to product formation (Fig. 3).[68] The activation barrier is again entirely entropic. IRC scans show that during SBM *via* **TS$_C$3-3b** and **TS$_C$3-3c** C–H bond formation is completed before Ti–F elimination starts noticeably.

Nucleophilic attack of H_{Ti} at C1 (S_NV) without Ti–F interaction *via* **TS$_B$3-IP1** (+10.5 kcal mol^{-1}) or with Ti–F interaction *via* **TS$_B$3-IP2** (+12.7 kcal mol^{-1}) results in the formation of contact ion pairs (CIP) **IP1** and **IP2** and the solvent separated ion pair (SIP) **IP4**, respectively (Fig. 4).[69] **TS$_B$3-IP1** is representative of several different, energetically close S_NV TS.[70] **IP4** is only 9.7 kcal mol^{-1} higher in free energy than **IP2** and can recombine to the HM intermediate (**5b**)[71] but can also decompose nearly barrierless.[72] A hypothetical '**IP3**' coming from **TS$_C$3-3b** is unstable. *Via* rotation, **IP1** leads equally to **IP2** and unstable '**IP3**', thus resulting in a statistical 1 : 1 ratio of **3a** and **3b**. An SET mechanism should be excluded based on the low electron affinity of perfluorinated olefins compared to perfluorinated arenes (see also studies for **4** next page).

Comparison of 1st TS geometries for 3

First steps in the different possible HDF mechanisms are irreversible thus pathway competition is given by TS $\Delta\Delta G^{\ddagger}$. All TS shown in Table 3 and Fig. 5 are energetically very early and purely entropic as a result of TS-formation out of two independent, yet almost unchanged, molecules ($\Delta G^{\ddagger}$ 8.5–12.7 kcal mol^{-1} from the separated reactants, $\Delta H^{\ddagger}$ −6.7 to −1.2 kcal mol^{-1}). **TS$_A$3-5d** and **TS$_C$3-3c** show only minimal changes in geometry from the isolated reactants.

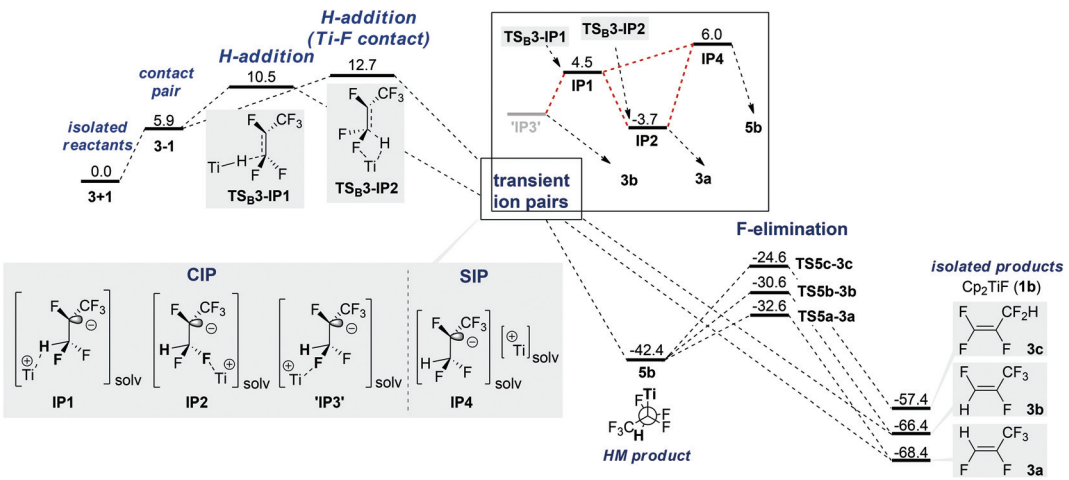

Fig. 4 PES for S_NV pathways for HDF of **3** (ΔG in kcal mol^{-1}, T = 298 K, 1 bar, in THF).

Open Access Article. Published on 18 August 2016. Downloaded on 11/12/2024 11:02:41 PM.
This article is licensed under a Creative Commons Attribution-NonCommercial 3.0 Unported Licence.

Table 3 Selected bond distances and angles in reactants and transition states (in Å or °). Ordered by TS enthalpy (kcal mol^{-1})

	Ti–H	C–H	F–Ti/C–Ti	C=C	FC=CF	$\Delta H^{\ddagger}$
1	1.703					
3				1.326		
1–3	1.738	2.638	3.803	1.327	0	−5.2
TS$_B$3-IP2	1.802	1.722	2.347	1.349	24	−1.1
TS$_B$3-IP1	1.780	1.610	—	1.360	29	−1.2
TS$_C$3-3b	1.788	1.731	2.314	1.349	22	−1.4
TS$_C$3-3c	1.760	1.788	2.354	1.366	24	−3.3
TS$_A$3-5d	1.717	2.170	2.802	1.352	17	−6.7

TS Gibbs free energies follow the trend in the distance of both reactants (shorter distance, higher TS energy) as exemplified by the H_{Ti}–C (1.61–2.17 Å), F–Ti (or C–Ti) distances (2.31–2.80 Å) and Ti–H bonds (stretched by max. 0.1 Å); all other bonds are not elongated more than 0.08 Å compared to the isolated reactants. For all TS beginning rehybridization is observed as the F_{cis}–C=C–F_{cis} dihedral angle ranges between 17–29°; a full rehybridization from sp^2 to sp^3 would change the dihedral angle from 0 to 60°. Fig. 5 shows the beginning formation of a lone pair on C2 for the 1st TS. IRC scans show that for all pathways, H-addition is completed and the lone pair on C2 fully formed, before Ti–C bond formation or Ti–F elimination starts.

Pathway competition for 3

The analysis of the reaction mechanism by DFT calculations exhibits that three HDF pathways are active in the F/H-exchange of **3** with **1**. With the exception of S_NV with Ti–F contact (**TS$_C$3-IP2**), all TS are within ±2 kcal mol^{-1}, *i.e.* HM, SBM and S_NV are competitive mechanisms.

Each of these mechanisms has its preferred ratio of isomers (Table 4). Allylic products are predicted to be exclusively formed by 6c-SBM and not as assumed previously exclusively formed by HM.[73]

Experimental selectivities correspond to energy differences ($\Delta G = RT\ln(k1/k2)$, T = 298.15 K) between the reaction pathways of 0.2 kcal mol^{-1} (**3a** *vs.* **3b**) and 2.3 kcal mol^{-1} (**3a** *vs.* **3c**). DFT predicts those differences to be 2.0 kcal mol^{-1} *via* HM/E and 2.0 kcal mol^{-1} *via* 6c-SBM, respectively. DFT predictions in THF are only qualitatively correct for the **3a**/**3b** ratio *via* the energetically lowest HDF pathway HM/E. The only mechanism that is energetically close and yields a selectivity close to the experimentally observed one is S_NV. All TS for HDF of **3** are very early, show only limited catalyst/substrate interactions and are basically entropy driven TS (see Fig. 6). Additionally, six different S_NV TS were found for **3**.

It appears plausible that in all or some cases the TS found analysing the electronic energy PES is not identical with the one on the Gibbs free energy PES. This could affect the predicted ratio of **3a** (*via* HM and S_NV) and **3b** (*via* S_NV). Another possible explanation is that the functional M06-2X is not accurate enough or that despite out best efforts, we have not found the lowest TS of type **TS$_B$3-IP1**.

Table 4 Experimental *vs.* predicted isomer ratio in THF ($\Delta G^{\ddagger}$ in kcal mol^{-1}, 298 K) for HDF of **3**

Ratio (exp.)	**3a**/**3b**/**3c** = 28 : 14 : 1				
Mechanism	HM/E	4c-SBM	6c-SBM	S_NV	S_NV (Ti–F)
Product	**3a**/**3b**/**3c**	**3b** only	**3c** only	**3a**/**3b**	**3a** only
Ratio (DFT)	29 : 1 : 0	<1	1	1 : 1	0
$\Delta G^{\ddagger}$ (THF)	8.5	10.9	10.5	10.5	12.7

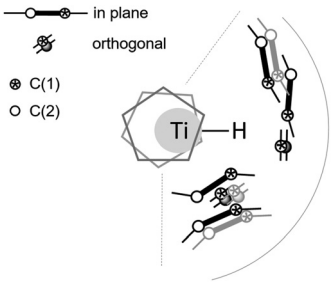

Fig. 6 Schematic overview of the plethora of possible HDF TS. Grey olefins differ in relative orientation wrt to the nearest black one, *e.g. cis vs. trans* C–F activation.

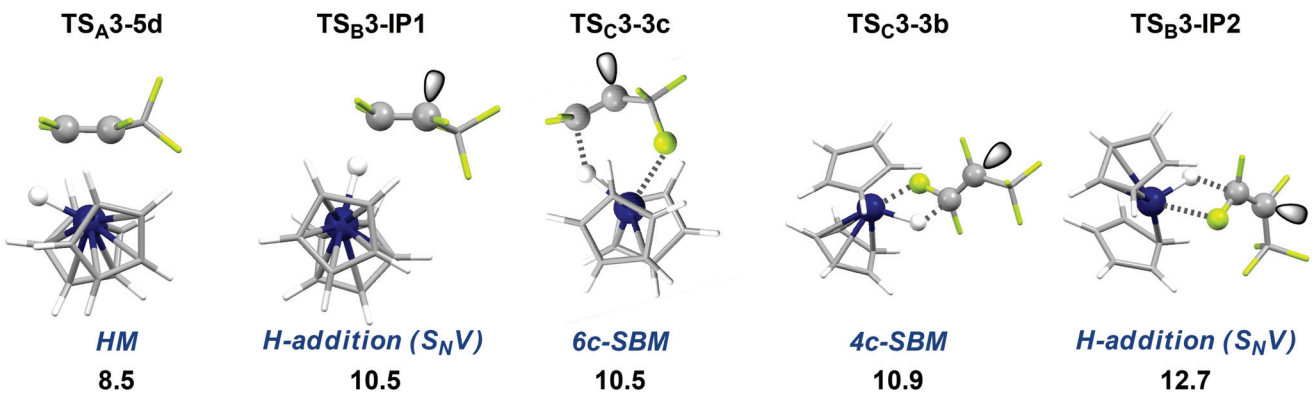

Fig. 5 Comparison of the first TS ($\Delta G^{\ddagger}$ in kcal mol^{-1}). Gibbs free energies of activation from the isolated reactants in THF (T = 298 K, 1 bar). Only the lowest TS of type **TS$_B$3-IP1** is shown.

This journal is © The Royal Society of Chemistry 2016

Open Access Article. Published on 18 August 2016. Downloaded on 11/12/2024 11:02:41 PM.
This article is licensed under a Creative Commons Attribution-NonCommercial 3.0 Unported Licence.

Experimental studies on HDF of 4

In order to study the different reactivities of various C–F bonds within one molecule we chose perfluoroallylbenzene (**4**) as an ideal substrate in the sense that it is the smallest possible molecule comprising vinylic, allylic and aromatic C–F bonds. Additionally, it features an extended low lying π*-orbital and HDF regioselectivity could help to clarify the potential role of SET type chemistry. The 1st HDF of **4** takes places at the C_3F_5-moiety and allylic (**4a,b**) and vinylic (**4c,d**) products are formed in a 3 : 2 ratio (Scheme 1), in striking contrast to other reported olefins where only trace amounts of the allylic product are observed. *E*/*Z* mixtures were obtained for both constitutional isomers and formation of the *E*-isomers is always preferred.

Increasing the amount of the catalyst or the reaction time or temperature leads to a second HDF step in the *para* position and formation of **4a′-d′** (Scheme 2).[74]

The eight new organofluorine compounds (**4a,a′,b,b′,c,c′,d,d′**) show distinct features in the ^{19}F and ^{1}H NMR spectra that allow for their unambiguous identification, see the Experimental section and ESI† for more details. The chemical shifts and coupling constants are only slightly affected by aromatic *para* H/F substitution, so that all resonances in the ^{19}F NMR are doubled except those for the missing *para*-F atom. Fig. 7–9 show some illustrative cut outs of a ^{19}F NMR spectra of a reaction mixture containing 1st and 2nd HDF products. Allylic HDF products show characteristic chemical shifts and coupling constants for the CF_2H-group around −124 ppm ($^2J_{FH}$ = 50.0 Hz for **4a** and $^2J_{FH}$ = 51.3 Hz for **4b**), additionally *trans* products have a characteristic large *trans*-F coupling constant ($^3J_{FF}$ = 138.0 Hz for **4a** and $^3J_{FF}$ = 136.0 Hz for **4c**) and the vinylic HDF products show the typical *gem*-H/F coupling constants ($^2J_{FH}$ = 71.5 Hz for **4c** and $^2J_{FH}$ = 68.9 Hz for **4d**). HDF for substrate **4**, similar to **3** (*E*/*Z* = 0.67), proceeds very unselectively.

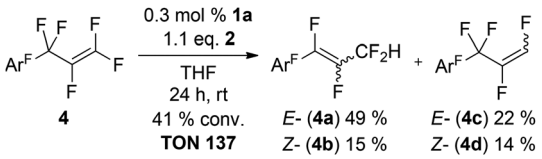

Scheme 1 Competing catalytic HDF of **4** (Ar_F = C_6F_5).

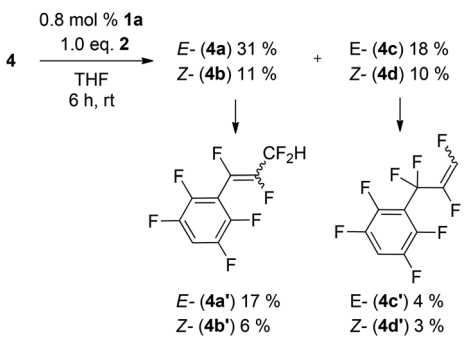

Scheme 2 2nd generation HDF products.

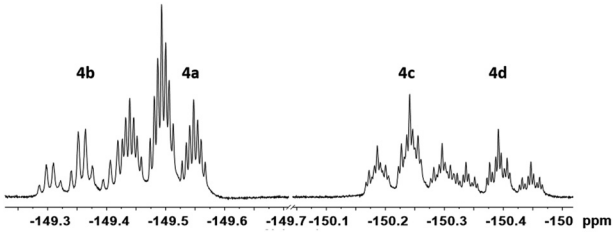

Fig. 7 ^{19}F NMR sequence of the *para*-F nuclei for 1st generation HDF products (−149.5 for **4a**, −149.4 for **4b**, −150.2 for **4c** and −150.4 ppm for **4d**).

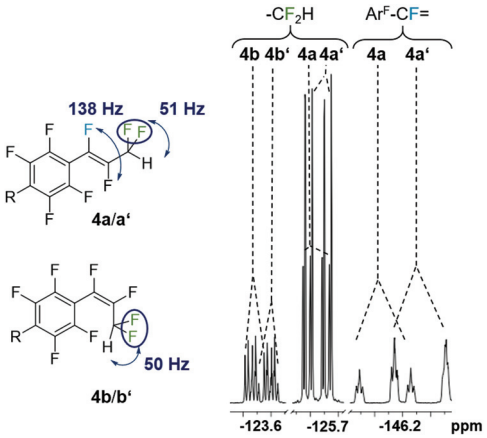

Fig. 8 Characteristic ^{19}F NMR resonances and coupling constants for 1st (**4a,b** with R = F) and 2nd generation allylic-HDF products (**4a′,b′** with R = H).

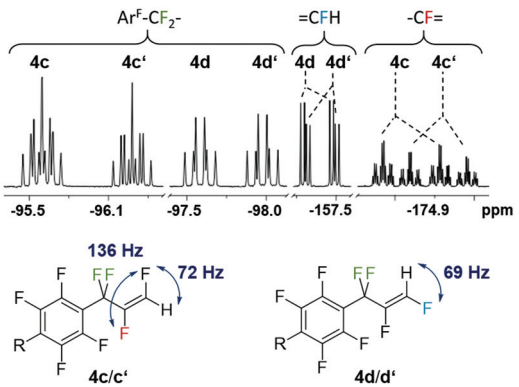

Fig. 9 Characteristic ^{19}F NMR resonances and coupling constants for 1st (**4c,d** with R = F) and 2nd generation vinylic-HDF products (**4c′,d′** with R = H).

DFT studies for 4

We assumed that the same mechanisms as just discussed for **3** could play a role for HDF of **4**. All TS were followed by IRC

Open Access Article. Published on 18 August 2016. Downloaded on 11/12/2024 11:02:41 PM.
This article is licensed under a Creative Commons Attribution-NonCommercial 3.0 Unported Licence.

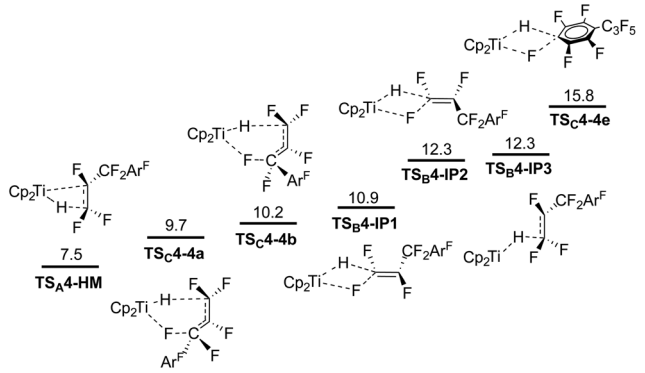

Fig. 10 Pathway competition for HDF of **4** (ΔG in kcal mol^{-1}, T = 298 K, 1 bar, in THF).

scans and lead to similar resting states (HM and S_NV pathways) or directly to the products (6c-SBM). Attack of **1** on C1, with or without a TiF contact in the TS, proceeds *via* S_NV and leads to a stable ion pair, regardless of a *cis* or *trans* approach (**TS_B4-IP1**, **TS_B4-IP2** and **TS_B4-IP3**; Fig. 10).[75] Both 6c-SBM TS (**TS_C4-4a** and **TS_C4-4b**) are favored over S_NV (with Ti–F contact). HM *via* **TS_A4-HM** is predicted to be the overall preferred pathway. All activation barriers are approx. 1 kcal mol^{-1} lower than they are for **3**. Within the HM pathway, the elimination TS leading to **4d** is heavily preferred (see the ESI†). The TS leading to allylic products (**4a** and **4b**) are 7 kcal, and the TS leading to **4c** are ~2.5 kcal mol^{-1} higher in energy.

DFT predictions are thus not in line with the experimentally observed selectivities as only **4d** should be formed. The aromatic C–F activation barrier is predicted to be significantly higher (but accessible for 2nd generation HDF) than the allylic and vinylic ones. SET was shown to be a possible mechanism for HDF of fluorinated arenes using late transition metals. However, the experimental selectivity in the 1st HDF product of **4** hints that SET cannot play a role here. While the low lying π*-LUMO of **4** is spread out through the whole molecule (Fig. 11), the most stable isomer of radical anion **4**$^{\bullet-}$ is **4A**$^{\bullet-}$ (negative charge and SOMO concentrated on the arene ring), and not **4B**$^{\bullet-}$ (calculated ΔG = +4.6 kcal mol^{-1}, negative charge and SOMO concentrated on C1 and C2 of the former alkene,

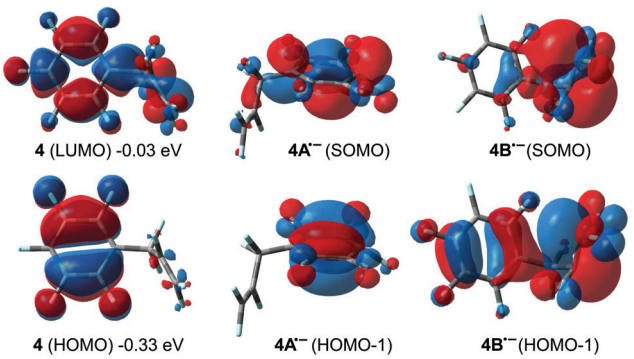

Fig. 11 Visualization of LUMO and HOMO for **4** and SOMO/HOMO–1 for **4**$^{\bullet-}$ and **4B**$^{\bullet-}$ (isovalue = 0.03).

respectively). However, 1st generation aromatic HDF products are not observed.

Suppressing S_NV reactivity

For both substrates (**3** and **4**), DFT is not able to correctly predict the product isomer ratios in THF. In both cases however, energetically low lying S_NV TS, which could be responsible for the low selectivity, were found. In order to suppress this S_NV reactivity *via* ion pairs we have changed the solvent from THF to toluene, both in the experiment and the calculations (Table 5). HDF of **3** in toluene exhibits an isomeric ratio of **3a** to **3b** to **3c** of 9 : 1 : 1, which is now completely in line with DFT results.[76] As expected the TS energy for **TS_B3-IP1** increases to +13.8 kcal mol^{-1} excluding this reaction pathway.[77]

A solvent change increases selectivity for **4** as well (Table 6). The initial test for other substrates, *e.g.* **5**, interestingly leads to multiple subsequent HDF steps.[78] We are currently optimizing reaction conditions for these substrates.

As mentioned earlier, **5** and **6** give one HDF product in major amounts (Table 1) even in polar solvents.[46] S_NV should be disfavored for HDF of **5** and **6** because ion pairs are destabilized as Fc or H groups are more electron donating than F, explaining the increase in selectivity, compared to **3**.[79]

Although solvent change (THF to toluene) lowers most barriers for activation, it decreases the TOF as it affects the rate limiting catalyst regeneration step, too.[54]

Similarly to **1**, DFT calculations for HDF of **3** using Cp_2ZrH_2 in toluene predict the *Z*-isomer **3a** but experimentally, Cp_2*ZrH_2 leads to the *E*-isomer **3b**.[55] This indicates that catalyst tuning should have an influence, and we subsequently tested the stoichiometric reaction of Cp^*_2TiH with **3**, which similarly favors the formation of the *E*-isomer (*E*/*Z* = 2.7). Previously, we tested selectivity of HDF of **3** with different catalysts in a polar solvent but the results presented here indicate that those tests should be repeated in a non-polar solvent to avoid S_NV reactivity.[46]

Table 5 Experimental *vs.* predicted isomer ratio in toluene ($\Delta G^{\ddagger}$ in kcal mol^{-1}, 298 K) for HDF of **3**

Ratio (exp.)	**3a**/**3b**/**3c** = 9 : 1 : 1				
Mechanism	HM/E	4c-SBM	6c-SBM	S_NV	S_NV (Ti–F)
Product	**3a**/**3b**/**3c**	**3b** only	**3c** only	**3a**/**3b**	**3a** only
Ratio (DFT)	12 : 1 : 0	>1	1	0 : 0	0
$\Delta G^{\ddagger}$ (tol.)	6.6	9.4	7.4	13.8	13.4

Table 6 Solvent effect on product selectivity

Substrate	**3**[39]	**4**	**3**	**4**	**5**
Solvent	Diglyme	THF	Toluene		
E : *Z*	1 : 1.5	2 : 1	1 : 9	100 : 1[a]	**5a**[b]

[a] Formation of C_6F_5–CH=CH–CF_3 (*E* (**4e**)/*Z* isomers) is observed. [b] Selective formation of CF_3–CH=CH_2 (**5a**).

This journal is © The Royal Society of Chemistry 2016

Open Access Article. Published on 18 August 2016. Downloaded on 11/12/2024 11:02:41 PM.
This article is licensed under a Creative Commons Attribution-NonCommercial 3.0 Unported Licence.

Conclusion

For the first time, a substrate (perfluoroallylbenzene) allowing conclusions for intramolecular competition of vinylic, allylic and aromatic was tested in HDF using **1**. A yet unmatched TON was observed but the reaction proceeds unselectively. Vinylic and allylic attacks are preferred over aromatic for the first HDF step but aromatic HDF becomes dominant in the subsequent step. SET likely plays no role in this reactivity.

DFT calculations provide previously unknown insight into Ti-catalyzed HDF reactions. In polar solvents, HM/E, 4-center-SBM, 6-center-SBM and S_NV are competitive reaction pathways. The latter one proceeds unselectively, which likely is responsible for low selectivities. Non-polar solvents can suppress S_NV reactivity leading to higher selectivity. Selectivity within the HM/E pathway is driven by product energy differences. 6c-SBM is preferred over SBM-4 reactivity.

We have recently shown that the barrier for regeneration is heavily dependent on the choice of silane. A combination of the right choice of silane and a non-polar solvent could therefore open routes to achieve highly selective HDF at low temperatures. This is a current focus in our laboratory.

Experimental section

All preparations were performed using standard Schlenk-type and vacuum-line techniques, or by working in an argon-filled glove box. Diglyme, THF and toluene were freshly distilled from sodium or potassium/benzophenone. **1a**, **2**, **4** (abcr) and **5** (SynQuest Labs) were obtained from commercially available sources and Cp^*_2TiH was synthesized analogous to a procedure reported for Cp'_2TiH (Cp′ = (1,2,3,4-tetramethyl-5-phenyl)cyclopentadienyl) starting from Cp^*_2TiMe.[80] **2** and **4** were distilled from calcium hydride and **1a** was sublimed prior to use. **3** (Solvay Fluor) was obtained free of charge and **3** and **5** were used as received.

Catalytic reactions

Reaction conditions and substrates are listed in Table S1 of the ESI.† A single-necked flask equipped with a PTFE valve was charged with **1a**, **2** and solvent. If no color change occurred the mixture was shortly heated with a heat gun (~10 s) until its color changed to green. Substrate addition: the frozen mixture was degassed prior to condensing the gaseous substrates. **4** was added *via* a syringe and degassed afterwards. By opening the valve the reaction was stopped, accompanied by a change of color from green to yellow; fluorobenzene (standard) was added and stirred for 5 min and NMR spectra were recorded.

Stoichiometric reaction

A single-necked flask equipped with a PTFE valve was charged with Cp^*_2TiH (20 mg, 0.06 mmol), dissolved in THF and an excess **3** was added. After a reaction time of one hour at room temperature the reaction was stopped by opening the vessel, fluorobenzene (standard) was added and stirred for 5 min and NMR spectra were recorded.

Hydrodefluorination products were identified by NMR spectroscopy, using literature data for **3a**,[81] **3b**[81] and **4e**.[82]

Data for HDF of 4. 4a: ^{1}H (400 MHz, C_6D_6): δ = 7.12 (1H, tdd, $^2J_{HF}$ = 51.3 Hz, $^3J_{HF}$ = 15.6 Hz, $^4J_{HF}$ = 2.5 Hz, –CF_2H) ppm; ^{19}F (376 MHz, C_6D_6): δ = −125.4 (2F, ddd, $^2J_{FH}$ = 51.2 Hz, $^3J_{FF}$ = 18.9 Hz, $^4J_{FF}$ = 1.3 Hz, –CF_2H), −136.8 (2F, m, *meta*-F_{arene}), −145.9 (1F, dtt, $^3J_{FF}$ = 138.0 Hz, $^4J_{FF}$ = 8.3 Hz, $^4J_{FF}$ = 1.4 Hz, Ar_F–CF═), −149.5 (1F, m, *para*-F_{arene}), −160.1 (2F, m, *ortho*-F_{arene}), −165.1 (1F, $^3J_{FF}$ = 138.0 Hz, ═CF–) ppm. **4b**: ^{1}H (400 MHz, C_6D_6): δ = 6.60 (1H, td, $^2J_{HF}$ = 50.0 Hz, $^3J_{HF}$ = 34.5 Hz, ═CFH) ppm; ^{19}F (376 MHz, C_6D_6): δ = −122.9 (1F, m, Ar_F–CF═), −123.8 (2F, ddd, $^2J_{FH}$ = 50.1 Hz, $^3J_{FF}$ = 19.7 Hz, $^4J_{FF}$ = 10.2 Hz, –CF_2H), −137.8 (2F, m, *meta*-F_{arene}), −149.4 (1F, m, *para*-F_{arene}), −157.5 (1F, ═CF–), −160.2 (2F, m, *ortho*-F_{arene}) ppm. **4c**: ^{1}H (400 MHz, C_6D_6): δ = 7.82 (1H, ddt, $^2J_{HF}$ = 68.5 Hz, $^3J_{HF}$ = 4.4 Hz, $^4J_{FH}$ = 1.4 Hz, ═CFH) ppm; ^{19}F (376 MHz, C_6D_6): δ = −95.6 (2F, m, Ar_F–CF_2–), −141.2 (2F, m, *meta*-F_{arene}), −150.2 (1F, ttt, $^3J_{FF}$ = 21.6 Hz, $^4J_{FF}$ = 5.3 Hz, $^6J_{FF}$ = 1.7 Hz, *para*-F_{arene}), −160.3 (2F, m, *ortho*-F_{arene}), −165.7 (1F, ddtt, $^2J_{FH}$ = 71.4 Hz, $^3J_{FF}$ = 136.0 Hz, $^4J_{FF}$ = 20.5 Hz, $^6J_{FF}$ = 2.3 Hz, ═CFH), −174.4 (1F, dtdt, $^3J_{FF}$ = 136.0 Hz, $^3J_{FF}$ = 18.1 Hz, $^3J_{FH}$ = 4.0 Hz, $^5J_{FF}$ = 3.6 Hz, –CF═) ppm. **4d**: ^{1}H (400 MHz, C_6D_6): δ = 7.51 (1H, ddt, $^2J_{HF}$ = 68.6 Hz, $^3J_{HF}$ = 15.4 Hz, $^4J_{FH}$ = 1.2 Hz, ═CFH) ppm; ^{19}F (376 MHz, C_6D_6): δ = −97.6 (2F, td, $^4J_{FF}$ = 25.8 Hz, $^3J_{FF}$ = 20.7 Hz, Ar_F–CF_2–), −140.6 (2F, m, *meta*-F_{arene}), −150.4 (1F, ttt, $^3J_{FF}$ = 21.9 Hz, $^4J_{FF}$ = 5.4 Hz, $^6J_{FF}$ = 1.7 Hz, *para*-F_{arene}), −153.8 (1F, m, –CF═), −157.1 (1F, dd, $^2J_{FH}$ = 68.9 Hz, $^3J_{FF}$ = 9.0 Hz, ═CFH), −159.9 (2F, m, *ortho*-F_{arene}) ppm. **4a′**: ^{1}H (400 MHz, C_6D_6): δ = 7.10 (1H, tdd, $^2J_{HF}$ = 51.3 Hz, $^3J_{HF}$ = 15.6 Hz, $^4J_{HF}$ = 2.5 Hz, –CF_2H) ppm; ^{19}F (376 MHz, C_6D_6): δ = −125.5 (2F, ddd, $^2J_{FH}$ = 51.2 Hz, $^3J_{FF}$ = 18.9 Hz, $^4J_{FF}$ = 1.3 Hz, –CF_2H), −137.0 (2F, m, *meta*-F_{arene}), −146.0 (1F, dtt, $^3J_{FF}$ = 138.0 Hz, $^4J_{FF}$ = 8.3 Hz, $^4J_{FF}$ = 1.4 Hz, Ar_F–CF═), −160.8 (2F, m, *ortho*-F_{arene}), −165.3 (1F, $^3J_{FF}$ = 138.0 Hz, ═CF–) ppm. **4b′**: ^{1}H (400 MHz, C_6D_6): δ = 6.55 (1H, tdd, $^2J_{HF}$ = 50.3 Hz, $^3J_{HF}$ = 15.6 Hz, $^4J_{HF}$ = 2.5 Hz, –CF_2H) ppm; ^{19}F (376 MHz, C_6D_6): δ = −123.1(1F, m, Ar_F–CF═), −123.7 (2F, ddd, $^2J_{FH}$ = 51.2 Hz, $^3J_{FF}$ = 21.2 Hz, $^4J_{FF}$ = 7.8 Hz, –CF_2H), −137.1 (2F, m, *meta*-F_{arene}), −154.8 (1F, m, ═CF–), −160.3 (2F, m, *ortho*-F_{arene}) ppm. **4c′**: ^{1}H (400 MHz, C_6D_6): δ = 7.80 (1H, ddt, $^2J_{HF}$ = 68.5 Hz, $^3J_{HF}$ = 4.4 Hz, $^4J_{FH}$ = 1.4 Hz, ═CFH) ppm; ^{19}F (376 MHz, C_6D_6): δ = −96.3 (2F, m, Ar_F–CF_2–), −141.4 (2F, m, *meta*-F_{arene}), −160.8 (2F, m, *ortho*-F_{arene}), −166.0 (1F, ddtt, $^2J_{FH}$ = 71.4 Hz, $^3J_{FF}$ = 136.0 Hz, $^4J_{FF}$ = 20.5 Hz, $^6J_{FF}$ = 2.3 Hz, ═CFH), −174.9 (1F, dtdt, $^3J_{FF}$ = 136.0 Hz, $^3J_{FF}$ = 18.1 Hz, $^3J_{FH}$ = 4.0 Hz, $^5J_{FF}$ = 3.6 Hz, –CF═) ppm. **4d′**: ^{1}H (400 MHz, C_6D_6): δ = 7.50 (1H, ddt, $^2J_{HF}$ = 68.6 Hz, $^3J_{HF}$ = 15.4 Hz, $^4J_{FH}$ = 1.2 Hz, ═CFH) ppm; ^{19}F (376 MHz, C_6D_6): δ = −97.9 (2F, td, $^4J_{FF}$ = 25.8 Hz, $^3J_{FF}$ = 20.7 Hz, Ar_F–CF_2–), −140.7 (2F, m, *meta*-F_{arene}), −154.0 (1F, m, –CF═), −157.2 (1F, dd, $^2J_{FH}$ = 68.9 Hz, $^3J_{FF}$ = 9.0 Hz, ═CFH), −160.1 (2F, m, *ortho*-F_{arene}) ppm.

GC-MS (EI, eV): m/z = 279.8 M^+ (4.43, 4.51, 4.58 min; **4a–d**), 261.7 M^+ (5.20, 5.24, 5.30; **4a′–d′**).

Computational details

All structures were fully optimized at the M06-2X(PCM)[83]/6-31+(2d,p) level of theory using Gaussian 09[57] coupled to an

Open Access Article. Published on 18 August 2016. Downloaded on 11/12/2024 11:02:41 PM.
This article is licensed under a Creative Commons Attribution-NonCommercial 3.0 Unported Licence.

external optimizer (PQS; convergence settings: DMAX 0.1, TOLG 0.0003, TOLE 0.00004, TOLD 0.0018)[84,85] instead of the internal Gaussian optimizer, using an ultrafine grid (Int(Grid = ultrafine)) and standard SCF convergence quality settings (Scf = tight) for Gaussian single point calculations. The nature of each stationary point was checked with an analytical second-derivative calculation (no imaginary frequency for minima, exactly one imaginary frequency for transition states, corresponding to the reaction coordinate) and the accuracy of the TS was confirmed with an IRC scan. S2 values for all doublet species are below 0.76. Solvent influence (THF, ε = 4.2457, toluene, ε = 2.3741) was modeled explicitly, using the polarizable continuum model (PCM) implemented in the Gaussian 09 software suite.

Transition states were located using a suitable guess and the Berny algorithm (Opt = TS)[86] or the Synchronous Transit-Guided Quasi-Newton (STQN) Method, developed by H. B. Schlegel and coworkers[87,88] (Opt = QST2 or QST3) or a relaxed potential energy scan to arrive at a suitable transition state guess, followed by a quasi-Newton or eigenvector-following algorithm to complete the optimization.

Vibrational analysis data derived at this level of theory were used to calculate thermal corrections (enthalpy and entropy, 298 K, 1 bar) for all species considered. Final single-point (SP) energies were calculated at the M06-2X(PCM)[89,90] level of theory employing triple-ζ Dunning basis sets (cc-pVTZ) from the EMSL basis set exchange library,[91,92] to minimize BSSE contributions,[93] including Grimmes' dispersion corrections for M06-2X (zero option in dftd3 standalone program).[94,95]

Acknowledgements

The authors would like to thank Prof. P. H. M. Budzelaar (U-Manitoba, Winnipeg) for generous donation of CPU time and valuable discussions on the manuscript. We thank Dr. Darina Heinrich for supportive data evaluation and helpful discussions. Support from the Deutsche Forschungsgemeinschaft (DFG) is gratefully acknowledged.

Notes and references

1 D. O'Hagan, *J. Fluorine Chem.*, 2010, **131**, 1071.
2 S. Purser, P. R. Moore, S. Swallow and V. Gouverneur, *Chem. Soc. Rev.*, 2008, **37**, 320.
3 I. S. R. Stenhagen, A. K. Kirjavainen, S. J. Forsback, C. G. Jørgensen, E. G. Robins, S. K. Luthra, O. Solin and V. Gouverneur, *Chem. Commun.*, 2013, **49**, 1386.
4 M. Tredwell and V. Gouverneur, *Angew. Chem., Int. Ed.*, 2012, **51**, 11426.
5 E. Lee, A. S. Kamlet, D. C. Powers, C. N. Neumann, G. B. Boursalian, T. Furuya, D. C. Choi, J. M. Hooker and T. Ritter, *Science*, 2011, **334**, 639.
6 J.-P. Bégué and D. Bonnet-Delpon, *Bioorganic and medicinal chemistry of fluorine*, John Wiley & Sons, Hoboken, N.J., 2008.
7 T. Nakajima and H. Groult, *Fluorinated materials for energy conversion*, Elsevier, Amsterdam, San Diego, CA, Oxford, 2005.
8 B. Ameduri and B. Boutevin, *Well-Architectured Fluoropolymers: Synthesis, Properties and Applications*, Elsevier Science, 2004.
9 A. McCulloch, *J. Fluorine Chem.*, 2003, **123**, 21.
10 M. P. Krafft and J. G. Riess, *J. Polym. Sci., Part A: Polym. Chem.*, 2007, **45**, 1185.
11 P. Kirsch, *Modern Fluoroorganic Chemistry*, Wiley-VCH Verlag GmbH & Co. KGaA, Weinheim, Germany, 2013.
12 K. Reichenbächer, H. I. Süss and J. Hulliger, *Chem. Soc. Rev.*, 2005, **34**, 22.
13 D. O'Hagan, *Chem. Soc. Rev.*, 2008, **37**, 308.
14 E. Clot, O. Eisenstein, N. Jasim, S. A. Macgregor, J. E. McGrady and R. N. Perutz, *Acc. Chem. Res.*, 2011, **44**, 333.
15 T. Ahrens, J. Kohlmann, M. Ahrens and T. Braun, *Chem. Rev.*, 2015, **115**, 931.
16 M. F. Kuehnel, D. Lentz and T. Braun, *Angew. Chem., Int. Ed.*, 2013, **52**, 3328.
17 T. A. Unzner and T. Magauer, *Tetrahedron Lett.*, 2015, **56**, 877.
18 J. Weaver and S. Senaweera, *Tetrahedron*, 2014, **70**, 7413.
19 M. Ohashi, M. Shibata and S. Ogoshi, *Angew. Chem., Int. Ed.*, 2014, **53**, 13578.
20 C. L. Clark, J. J. Lockhart, P. E. Fanwick and S. C. Bart, *Chem. Commun.*, 2015, **51**, 14084.
21 H. Luo, G. Wu, S. Xu, K. Wang, C. Wu, Y. Zhang and J. Wang, *Chem. Commun.*, 2015, **51**, 13321.
22 S. I. Kalläne, M. Teltewskoi, T. Braun and B. Braun, *Organometallics*, 2015, **34**, 1156.
23 D. McKay, I. M. Riddlestone, S. A. Macgregor, M. F. Mahon and M. K. Whittlesey, *ACS Catal.*, 2015, **5**, 776.
24 B. Procacci, Y. Jiao, M. E. Evans, W. D. Jones, R. N. Perutz and A. C. Whitwood, *J. Am. Chem. Soc.*, 2015, **137**, 1258.
25 P. Tian, C. Feng and T.-P. Loh, *Nat. Commun.*, 2015, **6**, 7472.
26 M. F. Kuehnel, D. Lentz and T. Braun, *Angew. Chem., Int. Ed.*, 2013, **125**, 3412.
27 M. Klahn and U. Rosenthal, *Organometallics*, 2012, **31**, 1235.
28 M. K. Whittlesey and E. Peris, *ACS Catal.*, 2014, **4**, 3152.
29 J.-Y. Hu and J.-L. Zhang, *Top. Organomet. Chem.*, 2015, **52**, 143.
30 N. A. LaBerge and J. A. Love, *Top. Organomet. Chem.*, 2015, **52**, 55.
31 T. Braun, D. Noveski, M. Ahijado and F. Wehmeier, *Dalton Trans.*, 2007, 3820.
32 T. Braun, F. Wehmeier and K. Altenhöner, *Angew. Chem., Int. Ed.*, 2007, **46**, 5321.
33 R. D. Rieth, W. W. Brennessel and W. D. Jones, *Eur. J. Inorg. Chem.*, 2007, 2839.
34 R. J. Lindup, T. B. Marder, R. N. Perutz and A. C. Whitwood, *Chem. Commun.*, 2007, 3664.

 This journal is © The Royal Society of Chemistry 2016

Open Access Article. Published on 18 August 2016. Downloaded on 11/12/2024 11:02:41 PM.
This article is licensed under a Creative Commons Attribution-NonCommercial 3.0 Unported Licence.

35 U. Jäger-Fiedler, M. Klahn, P. Arndt, W. Baumann, A. Spannenberg, V. V. Burlakov and U. Rosenthal, *J. Mol. Catal. A: Chem.*, 2007, **261**, 184.
36 S. P. Reade, M. F. Mahon and M. K. Whittlesey, *J. Am. Chem. Soc.*, 2009, **131**, 1847.
37 D. Breyer, T. Braun and A. Penner, *Dalton Trans.*, 2010, **39**, 7513.
38 B. M. Kraft, E. Clot, O. Eisenstein, W. W. Brennessel and W. D. Jones, *J. Fluorine Chem.*, 2010, **131**, 1122.
39 M. F. Kühnel and D. Lentz, *Angew. Chem., Int. Ed.*, 2010, **49**, 2933.
40 J. A. Panetier, S. A. Macgregor and M. K. Whittlesey, *Angew. Chem., Int. Ed.*, 2011, **50**, 2783.
41 T. F. Beltrán, M. Feliz, R. Llusar, J. A. Mata and V. S. Safont, *Organometallics*, 2011, **30**, 290.
42 D. Breyer, T. Braun and P. Kläring, *Organometallics*, 2012, **31**, 1417.
43 J.-H. Zhan, H. Lv, Y. Yu and J.-L. Zhang, *Adv. Synth. Catal.*, 2012, **354**, 1529.
44 M. F. Kuehnel, T. Schlöder, S. Riedel, B. Nieto-Ortega, F. J. Ramírez, J. T. López Navarrete, J. Casado and D. Lentz, *Angew. Chem., Int. Ed.*, 2012, **51**, 2218.
45 P. Fischer, K. Götz, A. Eichhorn and U. Radius, *Organometallics*, 2012, **31**, 1374.
46 M. F. Kuehnel, P. Holstein, M. Kliche, J. Krüger, S. Matthies, D. Nitsch, J. Schutt, M. Sparenberg and D. Lentz, *Chem. – Eur. J.*, 2012, **18**, 10701.
47 S. Yow, S. J. Gates, A. J. P. White and M. R. Crimmin, *Angew. Chem., Int. Ed.*, 2012, **51**, 12559.
48 H. Lv, Y.-B. Cai and J.-L. Zhang, *Angew. Chem., Int. Ed.*, 2013, **52**, 3203.
49 J. Li, T. Zheng, H. Sun and X. Li, *Dalton Trans.*, 2013, **42**, 13048.
50 H. Lv, J.-H. Zhan, Y.-B. Cai, Y. Yu, B. Wang and J.-L. Zhang, *J. Am. Chem. Soc.*, 2012, **134**, 16216.
51 J. Vela, J. M. Smith, Y. Yu, N. A. Ketterer, C. J. Flaschenriem, R. J. Lachicotte and P. L. Holland, *J. Am. Chem. Soc.*, 2005, **127**, 7857.
52 A. D. Selmeczy, W. D. Jones, M. G. Partridge and R. N. Perutz, *Organometallics*, 1994, **13**, 522.
53 A. A. Peterson and K. McNeill, *Organometallics*, 2006, **25**, 4938.
54 C. Ehm, J. Krüger and D. Lentz, *Chem. – Eur. J.*, 2016, **22**, 9305.
55 E. Clot, C. Mégret, B. M. Kraft, O. Eisenstein and W. D. Jones, *J. Am. Chem. Soc.*, 2004, **126**, 5647.
56 M. F. Kühnel, Doctoral thesis, FU-Berlin, 2011.
57 M. J. Frisch, G. W. Trucks, H. B. Schlegel, G. E. Scuseria, M. A. Robb, J. R. Cheeseman, G. Scalmani, V. Barone, B. Mennucci, G. A. Petersson, H. Nakatsuji, M. Caricato, X. Li, H. P. Hratchian, A. F. Izmaylov, J. Bloino, G. Zheng, J. L. Sonnenberg, M. Hada, M. Ehara, K. Toyota, R. Fukuda, J. Hasegawa, M. Ishida, T. Nakajima, Y. Honda, O. Kitao, H. Nakai, T. Vreven, J. A. Montgomery Jr., J. E. Peralta, F. Ogliaro, M. Bearpark, J. J. Heyd, E. Brothers, K. N. Kudin, V. N. Staroverov, R. Kobayashi, J. Normand, K. Raghavachari, A. Rendell, J. C. Burant, S. S. Iyengar, J. Tomasi, M. Cossi, N. Rega, J. M. Millam, M. Klene, J. E. Knox, J. B. Cross, V. Bakken, C. Adamo, J. Jaramillo, R. Gomperts, R. E. Stratmann, O. Yazyev, A. J. Austin, R. Cammi, C. Pomelli, J. W. Ochterski, R. L. Martin, K. Morokuma, V. G. Zakrzewski, G. A. Voth, P. Salvador, J. J. Dannenberg, S. Dapprich, A. D. Daniels, Ö. Farkas, J. B. Foresman, J. V. Ortiz, J. Cioslowski and D. J. Fox, Gaussian, Inc., Wallingford CT, 2009.
58 Rehybridization of the SOMO allowing participation of an empty coordination site at **1** can occur in the TS however.
59 The SOMO is predominantly concentrated on the metal in all TS but some delocalization into the organic fragments occurs in some of them. See the ESI† for SOMO pictures.
60 C. F. Bernasconi and Z. Rappoport, *Acc. Chem. Res.*, 2009, **42**, 993.
61 The barrier for hydride attack at C2 is +6.8 kcal mol^{-1} higher than $\mathbf{TS_A3}$**–5d**.
62 D. Y. Curtin and M. C. Crew, *J. Am. Chem. Soc.*, 1955, **77**, 354.
63 Relative values are derived from absolute values from Fig. 1 *via* subtraction TS-RS or TS-separated products.
64 E. W. Kaiser and D. S. Pierce, *J. Phys. Chem. A*, 2015, **119**, 9000.
65 N. C. Craig and E. A. Entemann, *J. Am. Chem. Soc.*, 1961, **83**, 3047.
66 R. Kanakaraju, K. Senthilkumar and P. Kolandaivel, *J. Mol. Struct.*, 2002, **589–590**, 95.
67 C. Ehm and D. Lentz, *J. Phys. Chem. A*, 2010, **114**, 3609.
68 Attack at C2 has significantly higher barriers. See the ESI.†
69 S_NV has not been reported as a possible mechanism for HDF using zirconocenes. The relatively strong Zr–H bond compared to Ti–H might be responsible for this ($Cp^*_2ZrH_2$ 81.0 ± 0.5 *vs*. Cp_2TiH 71.7 kcal mol^{-1}).
70 We found at least six, differing in orientation of the Cp rings and olefin.
71 This would represent a two step hydrometallation pathway but would lead back to a very selective mechanism (elimination from Ti-alkyl species) which is not in line with experimental observations.
72 Despite multiple attempts we were not able to locate an elimination TS from **IP2** but comparison of IRC scans of $\mathbf{TS_C3}$**-3b** (F^--elimination) and $\mathbf{TS_B3}$**-IP2** (charge separation) indicates that subtle changes in the relative orientation of anions and cations in the SIP can lead to barrierless F-elimination.
73 Earlier, we rendered a 6-membered SBM TS not feasible based on experimentally observed Ti(III)-halide angles but considering that the TS are very early, angles at Ti(III) should not be important and 6c-SBM is predicted to be more feasible than each of the two 4c-SBM.
74 Additional information and enhanced spectra in the ESI.†
75 This implies that the anion $\mathbf{4H^-}$ is even more stable than the anion $\mathbf{3H^-}$.
76 DFT calculations were repeated in toluene. Experimental selectivities in toluene correspond to energy differences

Open Access Article. Published on 18 August 2016. Downloaded on 11/12/2024 11:02:41 PM.
This article is licensed under a Creative Commons Attribution-NonCommercial 3.0 Unported Licence.

of 1.5 kcal mol^{-1} (**3a** *vs*. **3b**) and 1.5 kcal mol^{-1} (**3a** *vs*. **3c**). DFT predicts 1.9 and 0.8 kcal mol^{-1}, respectively, assuming **3a** and **3b** stem from HM/E and **3c** from 6c-SBM.

77 The barrier for **TS_B3-IP2** is heavily affected by the choice of solvent which is not observed for the other TS.

78 Something that was also observed for 3,3,3-trifluoropropene and trifluoroethylene in diglyme (see ref. 46).

79 DFT correctly predicts preference for the *E*-isomer *via* HM/E (0.7 kcal mol^{-1} *vs*. 1.2 kcal mol^{-1} experimentally) in THF.

80 J. M. de Wolf, A. Meetsma and J. H. Teuben, *Organometallics*, 1995, **14**, 5466.

81 H. Koroniak, K. W. Palmer, W. R. Dolbier and H.-Q. Zhang, *Magn. Reson. Chem.*, 1993, **31**, 748.

82 J.-j. Ma, W.-b. Yi, G.-p. Lu and C. Cai, *Adv. Synth. Catal.*, 2015, **357**, 3447.

83 Y. Zhao and D. G. Truhlar, *Theor. Chem. Acc.*, 2008, 215.

84 J. Baker, *J. Comput. Chem.*, 1986, 385.

85 J. Baker, *PQS, 2.4*, Parallel Quantum Solutions, Fayetteville, AR, 2001.

86 The Berny algorithm was never completely published, see the Gaussian documentation for details.

87 C. Peng, P. Y. Ayala, H. B. Schlegel and M. J. Frisch, *J. Comput. Chem.*, 1996, **17**, 49.

88 C. Peng and H. B. Schlegel, *Isr. J. Chem.*, 1993, **33**, 449.

89 R. Raucoules, T. de Bruin, P. Raybaud and C. Adamo, *Organometallics*, 2009, **28**, 5358.

90 S. Tobisch and T. Ziegler, *J. Am. Chem. Soc.*, 2004, **126**, 9059.

91 D. Feller, *J. Comput. Chem.*, 1996, **17**, 1571.

92 K. L. Schuchardt, B. T. Didier, T. Elsethagen, L. Sun, V. Gurumoorthi, J. Chase, J. Li and T. L. Windus, *J. Chem. Inf. Model.*, 2007, **47**, 1045.

93 S. F. Boys and F. Bernardi, *Mol. Phys.*, 1970, **19**, 553.

94 S. Grimme, J. Antony, S. Ehrlich and H. Krieg, *J. Chem. Phys.*, 2010, **132**, 154104.

95 S. Grimme, R. Huenerbein and S. Ehrlich, *ChemPhysChem*, 2011, **12**, 1258.

This journal is © The Royal Society of Chemistry 2016